Int. J. Electrochem. Sci., 11 **(2016)** 621 - 639

International Journal of
ELECTROCHEMICAL
SCIENCE
www.electrochemsci.org

Electrochemical Deposition of Nickel Oxide Nanocatalyst on Anodically Pretreated Glassy Carbon and its Electrocatalytic Activity

A. M. Ghonim[1], *B. E. El-Anadouli*[1], *M. M. Saleh*[1,2,*]

[1]Department of Chemistry, Faculty of Science, Cairo University, Giza, Egypt
[2]Chemistry Department, College of Science, King Faisal University, Al-Hassa, Saudi Arabia.
[*]E-mail: mahmoudsaleh90@yahoo.com

Received: 5 January 2015 / *Accepted:* 18 March 2015 / *Published:* 1 December 2015

The effects of anodic oxidation of glassy carbon (GC) in H_2SO_4 and NaOH electrolytes on the electrodeposition of nickel oxide nanoparticles (NiO_x) and on the electrocatalytic activity of the GC/NiO_x electrode are studied. Cyclic voltammetry (CV), Tafel Plot, scanning electron microscopy (SEM) and energy dispersive X-ray spectroscopy (EDX) are used for characterization of the electrodes. The structural and electrochemical characteristic of GC/NiO_x (GC is unoxidized), GC_{OX-AC}/NiO_x (GC is oxidized in acid (0.1 M H_2SO_4)) and GC_{OX-AL}/NiO_x (GC is oxidized in alkali (0.1 M NaOH)) are different. While NiO_x nanoparticles deposited on GC_{OX-AC} reveal a bird-like shape, it shows semi-spherical shape with larger size when it is deposited on either GC or GC_{OX-AL}. Glucose electrooxidation in alkaline medium is used as a probe reaction to study and compare the electrocatalytic activity of the GC/NiO_x with GC_{ox} (GC is oxidized in acid or alkali). Enhancement of glucose oxidation on either GC_{OX-AC}/NiO_x or GC_{OX-AL}/NiO_x is evident. While glucose oxidation on either GC_{OX-AC}/NiO_x or GC_{OX-AL}/NiO_x, shows higher peak currents, it shows negative shifts in both the peak and onset potentials only on the GC_{OX-AL}/NiO_x. The enhancement and the difference in the catalytic activity on both GC_{OX-AC} /NiO_x and GC_{OX-AL}/NiO_x are discussed in the light of surface analysis of both electrodes compared to GC /NiO_x.

Keywords: Glassy carbon, Oxidized, Nickel oxide, Nanoparticles, Glucose

1. INTRODUCTION

The substrate effect is an important issue in studying the electrocatalytic properties of the modified electrodes directed to fuels cells. Electrochemical pretreatment of glassy carbon (GC) is performed by anodic oxidation [1,2], cathodic reduction [3] or potential cycling [4,5]. The above processes took place in different media, e.g., acidic or alkaline electrolytes. Anodic oxidation of GC in the different solutions was achieved in order to compare the resulting surface analysis and structure

[6,7]. The surface analysis includes the degree of roughness (surface area) and surface concentration of C-O functional groups. In this context and here in this article, we aim to study the impacts of anodic oxidation of GC in acidic and alkaline media on the electrodeposition of NiO_x nanoparticles on the GC electrode. The electrodeposition of NiO_x on the different substrates results in different activities of the NiO_x towards important electrocatalytic reaction such as glucose oxidation from alkaline solution.

Applications of metal and metal oxides (MO_x) include (but not limited to): direct energy conversion and high capacitance devices [8-11], batteries [12], and sensors for biological species [13-15]. For an example, nickel oxides, NiO_x were prepared by different procedures for possible electrochemical applications. In this context, the preparation procedures are applied on ordinary untreated glassy carbon (GC) electrode. Such preparation procedures can be: preparation of nickel oxide powder (e.g., by sol-gel) NiO_x followed by casting [16], electrochemical [17] and others [18,19]. The structural properties of the prepared metal oxide nanoparticles can determine the catalytic activity of the oxide [20,21]. Impacts of anodic pretreatment of glassy carbon (prior to NiO_x electrochemical deposition) on the electrochemical characteristics and catalytic activity of NiO_x nanoparticles have not been well documented [22]. The electrodeposition is widely applied on glassy carbon electrode. GC electrode is always pretreated by normal procedure including mechanical polishing and then surface cleaning via sonication. Several reports on glucose electrooxidation using transition metal oxides, including both bulk and nanostructures based electrodes, such as NiO_x have been cited [23]. It is well known that nickel and nickel hydroxide exhibit excellent electrocatalytic performance in alkaline medium [24]. Oxidation of GC is known to enhance its electrocatalytic properties towards many applications such as electrochemical oxidation of many organic molecules [27-30]. Some authors [28-30] studied oxidation of organic fuels on oxidized glassy carbon electrode modified with platinum nanoparticles. In those works, the enhancement of the oxidation of those fuels was attributed to the increase in the surface area and creation of C-O functional groups on the GC substrate. While the effects of GC pretreatment by anodic oxidation on the electrooxidation of some small organic molecules have been studied [28-30], none has studied such effects on the glucose electrocatalytic oxidation albeit of equal importance.

The purpose of the present study is to compare the impacts of the anodic oxidation in H_2SO_4 and NaOH on the surface and electrochemical characteristics of NiO_x and its electrochemical activity towards an important reaction such as glucose oxidation in alkaline solution. The catalyst is fabricated electrochemically and is characterized by SEM, EDX and cyclic voltammetry. To the best of our knowledge, and despite the large number of articles regarding the electrodeposition of nickel oxide nanoparticles on GC, the present article is a first work in studying the effects of the GC anodic pretreatment in both acid and alkaline solutions before the electrodeposition of important metal oxide such as NiO. The shape and size and consequently the electrocatalytic activity of the obtained NiO_x nanoparticles are dramatically affected by the way of pretreatment of the GC electrode.

2. EXPERIMENTAL

Analytical grade chemicals were purchased from Merck, Sigma Aldrich and they were used as received without further purification. Solutions were prepared using second distilled water.

An ordinary cell with a three-electrode configuration was used in this study. A platinum spiral wire and an Ag/AgCl/KCl (sat.) were employed as counter and reference electrodes, respectively. Electrochemical measurements were performed using an EG&G potentiostat (model 273A) operated with E-Chem 270 software. All potentials will be presented with respect to this reference electrode. The working electrode was a glassy carbon (d = 3.0 mm). It was cleaned by mechanical polishing with aqueous slurries of successively finer alumina powder (down to 0.06 μm) then washed thoroughly with second distilled water. Scanning electron microscope (SEM) images were taken using field emission scanning electron microscope, FE-SEM (FEI, QUANTA FEG 250).

GC was oxidized in 0.1 M of H_2SO_4 (denoted as GC_{OX-AC}) and in 0.1 M of NaOH (denoted as GC_{OX-AL}) at 1.0, 1.5 and 2.0 V for different time periods (60, 120, 300 s). The GC modification with NiO_x was achieved as follows: First, the potentiostatic deposition of metallic nickel on the working electrode (i.e., GC or GC_{OX}) from an aqueous solution of 0.1 M acetate buffer solution (ABS, pH = 4.0) containing 1 mM $Ni(NO_3)_2 \cdot 6H_2O$ by applying a constant potential of −1.0 V. Second is the passivation of the metallic Ni in 0.1 M phosphate buffer solution (PBS, pH = 7) by cycling the potential between −0.5 and 1 V for 10 cycles at a scan rate of 200 mV/s. Prior to each of the above steps (deposition and passivation), the electrode was rinsed in water to get rid of any contaminates from the previous step. The electrode was then activated for 20 cycles in 0.5 M NaOH solution in the potential range −0.2 to 0.6 V. Cyclic voltammetry for glucose oxidation on different electrodes were measured in potential range of -0.2 to 0.6 V from 0.5 M NaOH containing different concentrations of glucose. The CVs were repeated twice to confirm the reproducibility of the results.

3. RESULTS AND DISCUSSION

3.1. Morphological and Surface Study:

Current-time relations (*i-t*) for anodic oxidation of GC electrode in 0.1 M H_2SO_4 (A) and 0.1 M NaOH (B) at constant potential of 2 V for 60 s are shown in Fig. 1. The general features of the two curves are similar. The obtained high current at the beginning of the anodic oxidation (either in acidic or alkaline) was attributed to the charging of the double layer. The curves are similar to that obtained in literature for GC [31]. The current decreases to minimum values before it increase again to reach a certain level. The current reaches its saturation higher limit once the water oxidation process is catalyzed to its possible maximum extent corresponds to the activation of the electrode process towards water oxidation [32]. The current obtained under oxidation in the acid is higher than that obtained in the alkali. This may be explained if we include the fact that the increase in the GC surface area (more roughness) due to oxidation in acid solution is more than that obtained in the alkaline solution (*c.f.* Fig. 2). This is in accordance with literatures [6].

The SEM images (Fig. 2A-C) demonstrate the morphology of glassy carbon surface before (A) GC and after oxidation of the GC in 0.1 M of H_2SO_4 (B, GC_{OX-AC}) and 0.1 M of NaOH (C, GC_{OX-AL}), respectively at 2 V for 300 s. The roughness obtained for GC_{OX-AC} is higher than that of GC_{OX-AL}. This

may be attributed to the higher degree of penetration of the acid than of the alkali. This is in accordance with literatures [6].

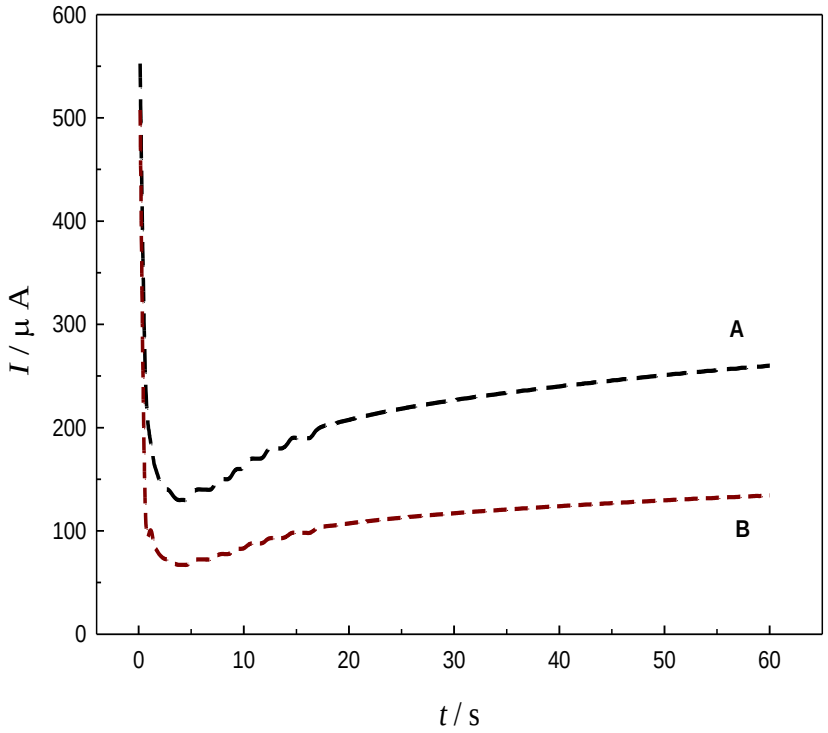

Figure 1. Monitoring of *i-t* for the oxidation of GC at anodic potential of 2.0 V in 0.1 M H_2SO_4 (A) and 0.1 M NaOH (B).

Table 1. Carbon and oxygen ratios obtained from EDX charts of GC and GC_{OX}. The GC_{ox} was prepared by oxidation of GC at 2 V for 300 s. in 0.1 M H_2SO_4 (GC_{OX-AC}) and 0.1 M NaOH (GC_{OX-AL}).

Type of electrode	GC	GC_{OX-AC}	GC_{OX-AL}
%C	97	90	92.3
%O	3	10	7.7

Table 1 lists the carbon and oxygen ratios extracted from EDX charts (not shown here) for the above three electrodes with the same details given in Fig. 2. The increase in the O% is attributed to the increase of surface concentration of the C-O functional groups on the GC surface due to surface oxidation. However, the increase in this ratio upon anodic oxidation in the acid is higher than that in the alkaline solution.

Figure 3(A-C) presents SEM images of the GC/NiO_x (A), GC_{ox-AC}/NiO_x (B) and GC_{OX-AL}/NiO_x (C). The microimages depict the morphology and particle size distribution of the NiO_x on the glassy carbon surface before (A) and after (B, C) activation of the surface in 0.1 M of H_2SO_4 and 0.1 M of

NaOH, respectively. Interestingly, the NiO_x nanoparticles electrodeposited on GC_{OX-AC} (B) is bearing a bird-like shape with average dimension of (70 x 650 nm ± 20 nm). The NiO_x particles obtained on GC (A) or GC_{OX-AL} (C) have larger size (average size of 150 and 100 nm (± 20 nm), respectively) with semi-spherical shape.

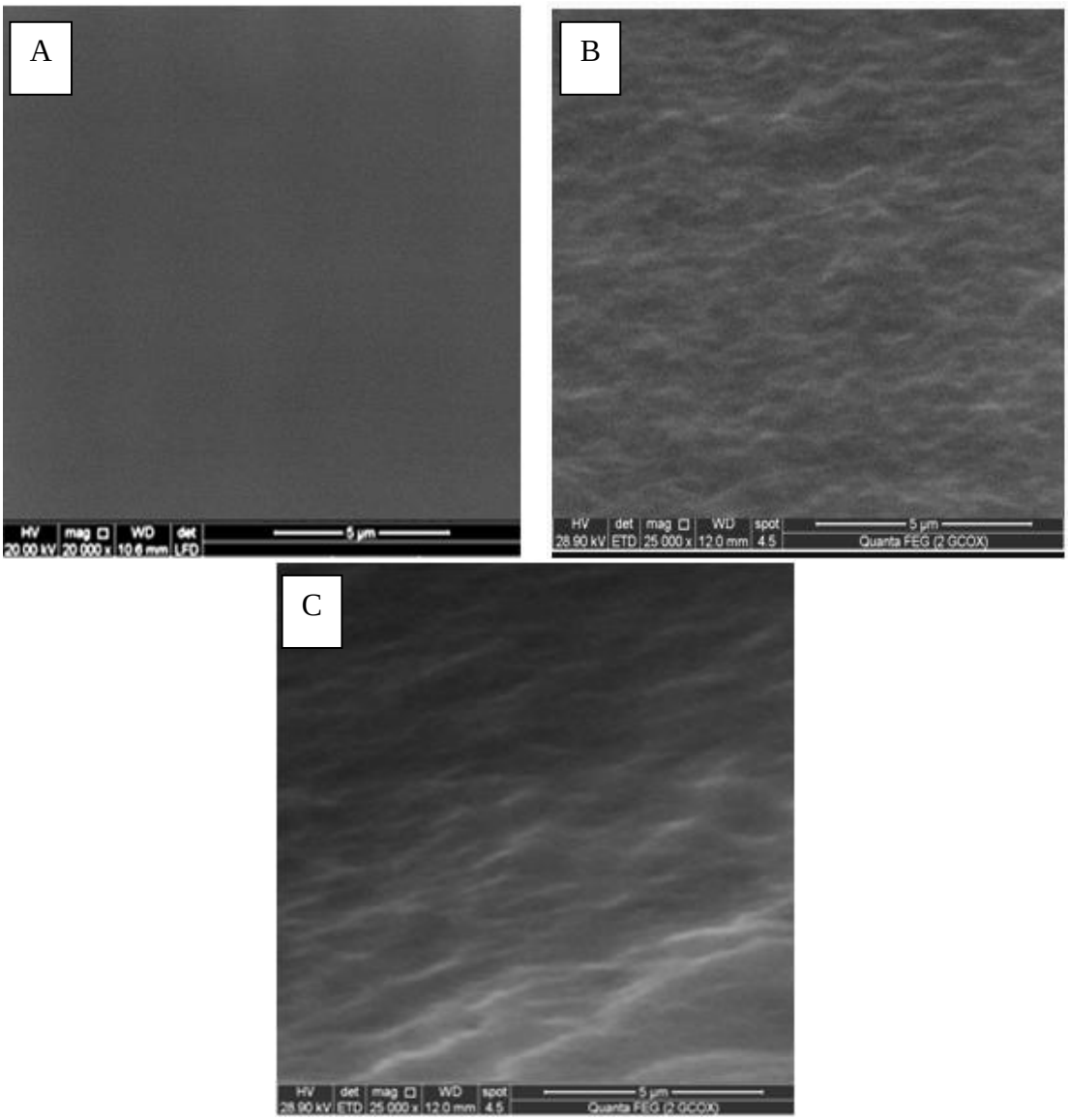

Figure 2. FE-SEM images of GC (A), GC_{OX-AC} (B) and GC_{OX-AL} (C). The GC_{OX-AC} and GC_{OX-AL} were prepared by oxidation of GC at 2 V in 0.1 M H_2SO_4 or NaOH for 300 s.

3.2. Impacts on the Electrochemical Characteristics:

The impacts of anodic oxidation of GC on the electrodeposition of NiO_x on the pretreated GC can be explained after considering the parameters listed in Table 2.

Table 2. Time (t_{dep}) required for electrodeposition of constant amount of Ni (Q = 15 mC in all cases) on glassy carbon pretreated by oxidation at different anodic potential, E_{anodic} in 0.1 M H_2SO_4 ($GC_{OX\text{-}AC}$) and 0.1 M NaOH ($GC_{OX\text{-}AL}$) for different time period, t_{anodic}.

t_{anodic} / s	E_{anodic} / V	t_{dep} /s	
		$GC_{OX\text{-}AC}$	$GC_{OX\text{-}AL}$
0	Untreated	240	240
60	1	130	155
	1.5	115	130
	2	95	105
120	1	110	140
	1.5	80	120
	2	55	85
300	1	80	110
	1.5	65	75
	2	45	60

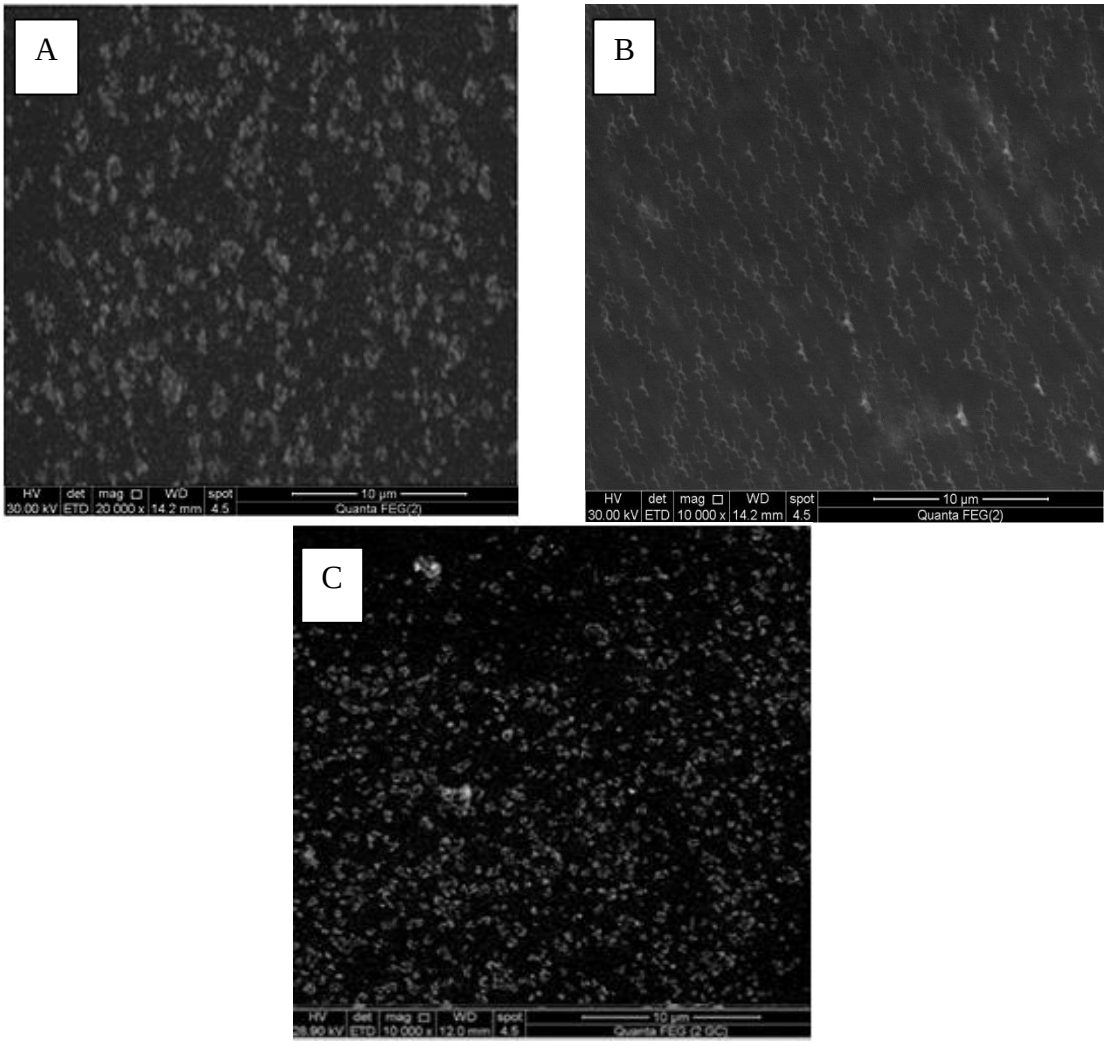

Figure 3. FE-SEM images of GC/NiO_x (GC is untreated) (A), $GC_{OX\text{-}AC}/NiO_x$ (B) and $GC_{OX\text{-}AL}/NiO_x$. Before NiO_x electrodeposition, the GC was oxidized at 2 V for 300 s in 0.1 M H_2SO_4 (B) and 0.1 M NaOH (C).

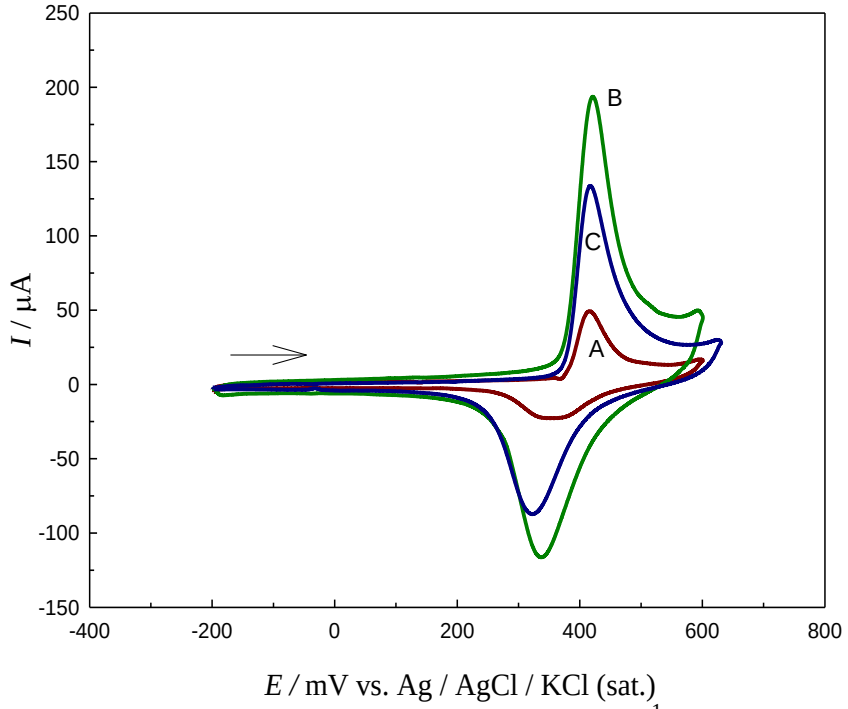

Figure 4. CVs in 0.5 M NaOH (blank) using scan rate of 100 mV s^{-1} for GC/NiO_x (A), $GC_{OX\text{-}AC}/NiO_x$ (B) and $GC_{OX\text{-}AL}/NiO_x$ (C) where GC was pretreated by oxidation at 2 V for 60 s in 0.1 M of H_2SO_4 (B), in 0.1 M of NaOH (C).

It shows the time required for deposition of a constant loading of Ni on untreated and pretreated GC at different conditions. The GC electrode was pretreated by oxidation at different anodic potentials, E_{anodic} for different time period, t_{anodic}. Constant loading of Ni corresponds to a constant electrodeposition charge, Q equals to 15 mC in our case. This amount of charge and assuming 100% columbic efficiency corresponds to a loading of Ni equal to ~ 0.065 mg cm^{-2}. The time required for deposition of the same loading of Ni (i.e., the same amount of Q) decreases with the oxidation potential, E_{anodic} and with the time period, t_{anodic} used in the GC oxidation in acid and alkali. The modification of the GC electrode with nanoparticles of NiO_x was performed as discussed in the experimental section. Three glassy carbon were used; one without activation (GC), GC after treatment at an anodic potential at different t_{dep} in 0.1 M H_2SO_4 ($GC_{ox\text{-}AC}$) or in 0.1 M NaOH ($GC_{OX\text{-}AL}$). Since the reaction rate increases with the increase in the electrode surface, hence the time required for electrodeposition of the constant loading of Ni decreases with the increase in the GC surface area (due to oxidation, see Fig. 2). This is clearly revealed from Table 2. We can easily note that (for an example), 45 s is required to pass the 15 mC at $GC_{OX\text{-}AC}$ (oxidized at 2 V for 300 s), 60 s at $GC_{OX\text{-}AL}$ (at the same oxidation conditions) and 240 s is required to pass the same amount of charge on the untreated GC electrode. This was attributed to the higher surface area and higher reactivity of the $GC_{OX\text{-}AC}$ and $GC_{OX\text{-}AL}$ compared to that of the untreated GC. Note that t_{dep} (at any t_{anodic} and E_{anodic}) for the $GC_{OX\text{-}AC}$ is lower than that of the $GC_{OX\text{-}AL}$ which indicates higher activity of the $GC_{OX\text{-}AC}$ compared to $GC_{OX\text{-}AL}$. This is consistence with the conclusions driven from the SEM images in Fig. 2 and the EDX data in Table 1.

Figure 4 shows characteristics CVs for GC/NiO_x, $GC_{OX–AC}$ /NiO_x and $GC_{OX–AL}$/NiO_x in 0.5 NaOH solution (blank). For the last two electrodes, before Ni deposition, the GC was subjected to anodic oxidation in 0.1 M H_2SO_4 or 0.1 M NaOH at 2V for 300 s. The figure reveals that the peak current for the redox couple ($Ni(OH)_2 \leftrightarrow NiOOH$) has the order: GC/$NiO_x$ < $GC_{OX–AL}$/NiO_x < $GC_{OX–AC}$/NiO_x for both anodic and cathodic peaks. This increase in the peak current is attributed to the increase in the substrate surface area which gives rise to the surface area of the NiO_x nanoparticles. Also, the increase in the surface concentration of C–O functional groups may facilitate the electron transfer for the nickel oxide redox couple. For instance, the anodic peak current at the GC_{OX-AC}/NiO_x increases to about four folds and at the GC_{OX-AL}/NiO_x, it increases to about three folds with respect to the untreated GC (i.e., GC/NiO_x). The surface concentration of the active nickel sites, Γ can be estimated from: $\Gamma = Q/nF$ [35,36], where Q (charge consumed in the $Ni^{2+} \rightarrow Ni^{3+}$ process) can be estimated from the area under the CV curve at scan rate of 5 mV s^{-1} for the above three electrodes. The value of Γ was found to be 0.63, 2.57 and 1.74 nmol cm^{-2} for GC/NiO_x, $GC_{OX–AC}$/NiO_x and $GC_{OX–AC}$/NiO_x, respectively. The values of Γ are consistent with the above conclusions.

The anodic and cathodic scans for the nickel hydroxide electrode substrate, are known to produce various phases of the hydroxide namely, β-$Ni(OH)_2$, α-$Ni(OH)_2$, β-NiOOH, and γ-NiOOH [33]. It is well known that the formation of γ-NiOOH phase is associated with swelling of the nickel film and consequently, microcracks and disintegrates may be formed. Therefore, β-NiOOH phase is expected to be a better electroactive material for high electrochemical performance in alkaline solution [34]. There is also a possibility of preferential formation of β-NiOOH at the GC_{OX} but not on GC. The Ni(II)/Ni(III) conversions occur via two pathways, by a proton diffusion mechanism in which β-NiOOH is likely formed (Eq. 1), and by solvent mechanism in which γ-NiOOH is formed through the diffusion of OH^- (Eq. 2) [37,38]

$$Ni(OH)_2 \leftrightarrow NiOOH + H^+ + e^- \quad (1)$$

$$Ni(OH)_2 + OH^- \leftrightarrow NiOOH + H_2O + e^- \quad (2)$$

In the next section we are going to study the impacts of the above findings on the electrocatalytic properties of NiO_x towards glucose oxidation in alkaline solution .

To confirm the fact that the amount of the electrodeposited Ni on either GC or GC_{OX} is a fixed amount, one can consider the followings. The total passed charge during Ni electrodeposition, Q_{total} is the sum of the charge passed for hydrogen evolution reaction, Q_{H2} and the charge passed for the Ni deposition, Q_{Ni} such that;

$$Q_{total} = Q_{H2} + Q_{Ni} = Const. = 15 \text{ mC} \quad (3)$$

Note that $Q_{H2} = I_{H2} \, x \, t_{dep}$ and $Q_{Ni} = I_{H2} \, x \, t_{dep}$. Upon anodic oxidation of the GC in either acid or alkali, the rate of the electrochemical reaction on GC_{OX} increases due to reasons discussed above. Hence, both I_{H2} and I_{Ni} increases but the time required for both processes which support that currents decreases since $Q_{total} = (I_{H2} + I_{Ni}) \, x \, t_{dep}$ = Constant. That is to say, both I_{H2} and I_{Ni} increases (due anodic oxidation of GC) but t_{dep} decreases (see Table 2). We ran two electrodeposition experiments for GC and GC_{OX} at -1.0 V for specific time, t_{dep}. The latter time was chosen from Table 2 for the case of E_{anodic} = 2 V for 300 s in the acid medium. First experiment was done by recording *I-t* curve at -1.0V

on GC from blank only (i.e., PBS, pH = 7) (see Experimental section) and the other experiment was done similarly but from 1mM $Ni(NO_3)_2$ in PBS, pH = 7.

Table 3. Anodic peak current, I_{pa}, cathodic peak current, I_{pc}, the ratio (I_{pc}/I_{pa}) and the surface concentration of Ni sites, Γ for GC/NiO_x, $GC_{OX\text{-}AC}/NiO_x$ and $GC_{OX\text{-}AL}/NiO_x$ in 0.5 M NaOH (blank). The GC was pretreated in different solutions and at different anodic potential, E_{anodic} and different time period of anodic oxidation, t_{anodic}.

t_{anodic}/s	E_{anodic} / V	$GC_{OX\text{-}AC}/NiO_x$				$GC_{OX\text{-}AL}/NiO_x$			
		I_{pa} /μA	I_{pc} /μA	Ratio I_{pc}/I_{pa}	Γ/ nmol cm^{-2}	I_{pa} /μA	I_{pc} /μA	Ratio I_{pc}/I_{pa}	Γ/ nm cm^{-2}
0	Untreated	47	22	0.46	0.63	47	22	0.46	0.63
60	1	71	33	0.473	1.09	53	34	0.630	0.91
	1.5	78	42	0.523	1.09	77	49	0.646	1.04
	2	103	50	0.484	1.22	86	50	0.586	1.02
120	1	84	40	0.473	0.97	79	48	0.600	1.37
	1.5	103	78	0.751	1.55	95	49	0.520	1.46
	2	130	79	0.606	1.97	105	60	0.577	1.24
300	1	103	62	0.598	1.67	106	68	0.638	1.51
	1.5	144	109	0.758	2.17	109	72	0.656	1.44
	2	192	115	0.600	2.57	133	87	0.654	1.74

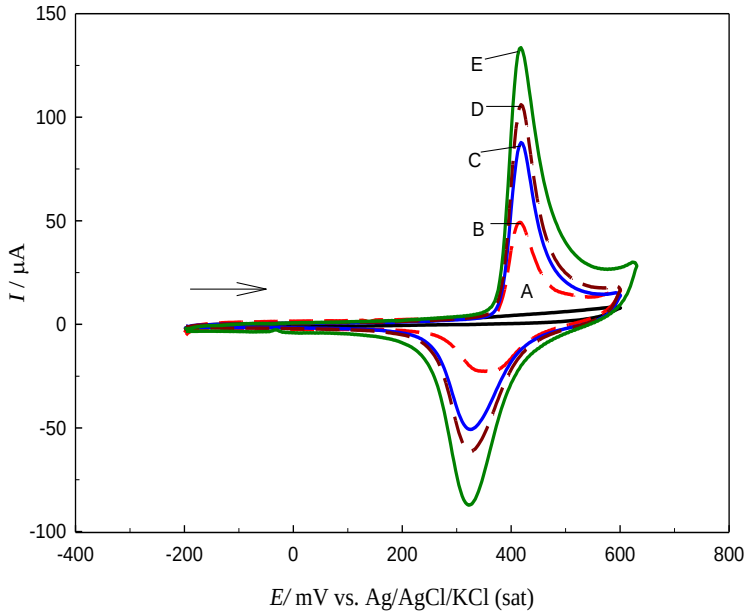

Figure 5. CV responses in 0.5 M NaOH using scan rate of 100 mV s^{-1} at GC (A), GC/NiO_x (B) and $GC_{OX\text{-}AL}$ /NiO_x (C-E) where GC was pretreated by oxidation at 2 V for 60 s (C), 120 s (D), 300 s (E) in 0.1 M NaOH.

The measured current in the 1st and 2nd experiment is I_{H2} (blank) and (I_{H2} + I_{Ni}) (presence of Ni^{2+}), respectively. It was found that to pass the 15 mC (total fixed charge) a Q_{H2} = 1.02 mC and Q_{Ni} = 15.0 – 1.02 = 13.98 mC were passed on the GC electrode. Those values were found to be; Q_{H2} = 1.2 mC and Q_{Ni} = 13.8 mC for GC_{OX} (oxidized in 0.1 M H_2SO_4 for 300 s and at 2 V). Similar values were obtained for anodic oxidation in alkali. We may conclude that the large differences in the peak current (*i.e.*, enhancement of the Ni(II)/Ni(III) redox couple) shown in Figs. 4 and 5 and in Table 3 are not attributed to a possible difference in the NiO_x loading but rather to the differences in anodic pretreatment of the GC electrode.

Figure 5 depicts CVs responses for A) GC, B) GC/NiO_x and C-E) GC_{OX-AL} /NiO_x in 0.5 M NaOH (blank) at scan rate of 100 mV s^{-1}. The GC_{OX-AL} /NiO_x was prepared by electrodeposition of NiO_x on GC_{OX-AL} previously prepared by anodic oxidation of GC in 0.1 M NaOH at E_{anodic} of 2 V for 60 (C), 120 (D) and 300 s (E). As the time of anodic oxidation, t_{anodic} increases, the peak current of the redox couple $Ni(OH)_2 \leftrightarrow NiOOH$ increases. Similar CVs were collected for GC_{OX-AC} /NiO_x and GC_{OX-AL} /NiO_x where the GC was anodically oxidized at different E_{anodic} and t_{anodic} prior to NiO_x deposition. Analysis of the above collected CVs was performed to extract important electrochemical parameters. Table 3 lists such parameters. These include; the anodic and cathodic peak current of the $Ni(OH)_2$/NiOOH redox couple, I_{Pa} and I_{Pc}, respectively, ratio of the peak currents (I_{Pc}/I_{Pa}) and the surface concentration of Ni active sites, Γ. As E_{anodic} and/or t_{anodic} increases, the peak current (especially I_{pa}) increases and the ratio I_{Pc}/I_{Pa} increases and becomes more closer to unity compared to those of the GC/NiO_x. The above results imply that the reactivity and reversibility of the $Ni(OH)_2$/NiOOH redox couple increases [39,40]. Also, the surface concentration, Γ increases with E_{anodic} and/or t_{anodic} pointing to the increase in the concentration of the Ni active species in the matrix.

3.3. Electrocatalytic activity:

Figure 6 shows LSV responses for glucose oxidation at different electrodes from 0.5 M NaOH containing 20 mM glucose solutions at scan rate of 100 mV s^{-1}. The electrodes are; A) GC, B) GC_{OX-AC}, C) GC_{OX-AL} , D) GC /NiO_x, E) GC_{OX-AC} /NiO_x F) GC_{OX-AL}/NiO_x. The last two electrodes (curves E and F) were prepared by anodic oxidation of GC electrode at 2 V for 300 s in 0.1M H_2SO_4 and 0.1 M NaOH, respectively.

The first three electrodes ((A) GC, B) GC_{OX-AC}, and C) GC_{OX-AL}) do not show any significant catalytic action towards glucose oxidation. The figure demonstrates that both GC_{OX-AC}/NiO_x (curve E) and GC_{OX-Al} /NiO_x (curve F) show dramatic increases in the peak current of glucose oxidation compared to GC/NiO_x (curve D). A negative shift in the onset potential, E_{onset} of glucose oxidation is obtained in case of GC_{OX-AL}/NiO_x. For instance, E_{onset} of glucose oxidation is 0.20 and 0.35 V for GC_{OX-AL}/NiO_x and GC/NiO_x, respectively. In the other hand, the E_{onset} does not change at the GC_{OX-AC}/NiO_x but the peak current is higher than that obtained on GC_{OX-AL}/NiO_x. That is to say, while anodic oxidation of GC in acidic solution results in an increase in the peak current of glucose oxidation, it affects both peak current and E_{onset} upon anodic treatment in alkaline solution.

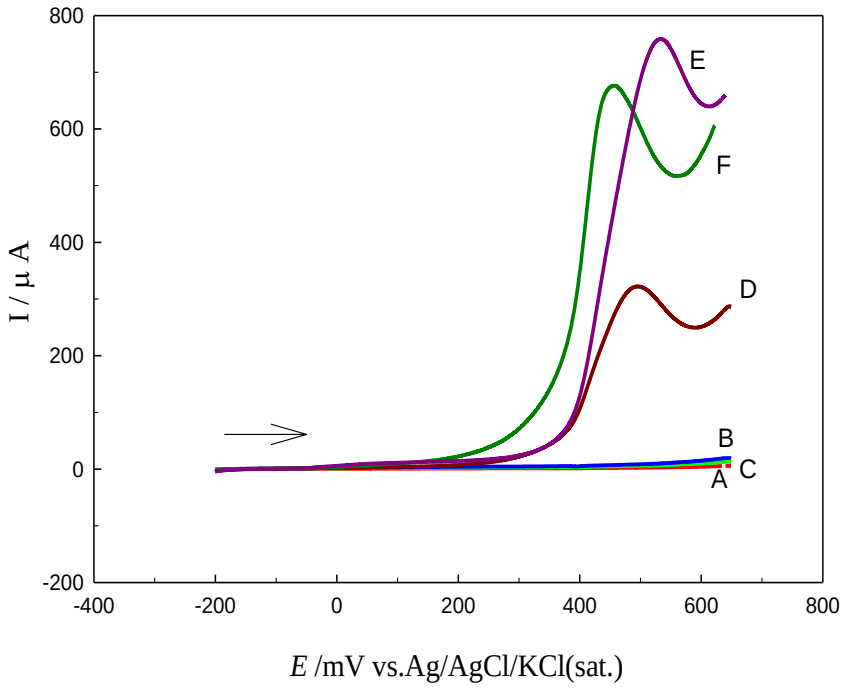

Figure 6. LSV in 0.5 M NaOH solution containing of 20 mM glucose. The scan rate is 100 mV s^{-1} at GC(a), GCox-AC (B), GCox-AL(C), GC/NiO_x (D), GC_{OX-AC}/NiO_x (E), GC_{OX-AL}/NiO_x (F).

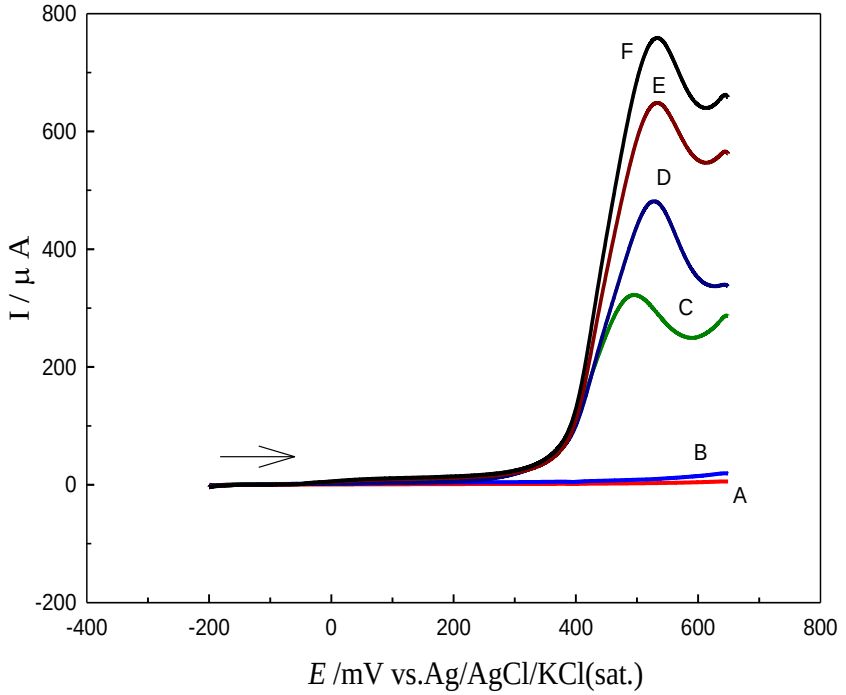

Figure 7. LSV in 0.5 M NaOH solution containing of 20 mM glucose. The scan rate is 100 mV s^{-1} at GC (A), GC_{OX-AC} (B), GC/NiO_x (C), GC_{OX-AC}/NiO_x (D-F) where GC was pretreated by oxidation at 2 V for 60 s (D), 120 s (E), 300 s (F) in 0.1 M H_2SO_4.

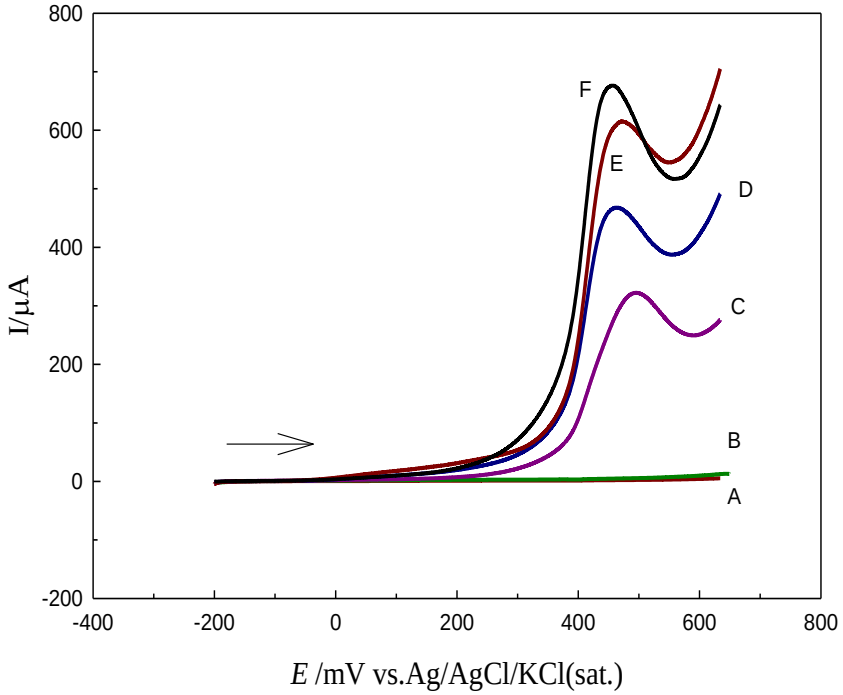

Figure 8. LSV in 0.5 M NaOH solution containing of 20 mM glucose. The scan rate is 100 mV s^{-1} at GC (A), GC_{OX-AL}(B), GC/NiO_x (C) and GC_{OX-AL}/NiO_x (D-F) where GC was pretreated by oxidation at 2 V for 60 s (D), 120 s (E), 300 s (F) in 0.1 M NaOH.

The negative shift in E_{onset} points to the easiness and facilitated oxidation of glucose on GC_{OX-AL}/NiO_x. In the other hand the increase in the peak current may be attributed to the GC surface modification and the increase in surface area of the GC.

Figure 7 and 8 show LSV responses for glucose oxidation at GC_{OX-AC}/NiO_x and GC_{OX-AL}/NiO_x, respectively in 0.5 M NaOH containing 20 mM glucose solution at scan rate of 100 mV s^{-1}. In both figures, the GC was oxidized anodically at 2 V for different time periods in 0.1 M H_2SO_4 (Fig. 7) and in 0.1 M NaOH (Fig. 8) before NiO_x deposition. It has been shown that the value of anodic potential, E_{anodic} and t_{anodic} have significant effects on the surface modification of the GC. On both electrodes (GC_{OX-AC}/NiO_x and GC_{OX-AL}/NiO_x), the peak current of glucose oxidation increases as the time period of anodic oxidation increases. However, for the GC_{OX-AL}/NiO_x, the E_{onset} and peak potential, E_p shifts to more negative values.

Figures 9 and 10 show CV responses for glucose oxidation on GC_{OX-AC}/NiO_x and GC_{OX-AL}/NiO_x from 0.5 M NaOH containing 20 mM glucose. The GC in the two electrodes was subjected to anodic oxidation for 300 s at different anodic potentials. The peak current increases with the E_{anodic} in both cases. However, the E_{onset} and E_p of glucose oxidation shift to more –ve values in case of GC_{OX-AL}/NiO_x. The features in Figs. 9 and 10 are similar to those shown in Figs. 7 and 8. The same amount of charge (Q = 15 mC) was used to deposit Ni on the different electrodes.

Similar LSVs obtained in Figs.7-10 were measured for glucose oxidation on the different electrodes at different conditions of GC anodic oxidation. The figures were analyzed and important electrochemical parameters are extracted.

Table 4. Peak current, I_p, peak potential, E_p and onset potential, E_{onset} of glucose oxidation on GC/NiO_x, $GC_{OX\text{-}AC}/NiO_x$ and $GC_{OX\text{-}AL}/NiO_x$ at different anodic potential, E_{anodic} and for different time period, t_{anodic} of GC oxidation.

t_{anodic} / s	E_{anodic} / V	I_p /µA		E_p / V	
		$GC_{OX\text{-}AC}/NiO_x$	$GC_{OX\text{-}AL}/NiO_x$	$GC_{OX\text{-}AC}/NiO_x$	$GC_{OX\text{-}AL}/NiO_x$
0	GC/NiO_x Untreated	325	325	493	493
60	1	410	390	537	498
	1.5	460	405	532	497
	2	485	450	526	458
120	1	455	430	537	493
	1.5	560	510	526	492
	2	635	585	531	470
300	1	485	456	520	485
	1.5	634	585	526	475
	2	765	680	534	456

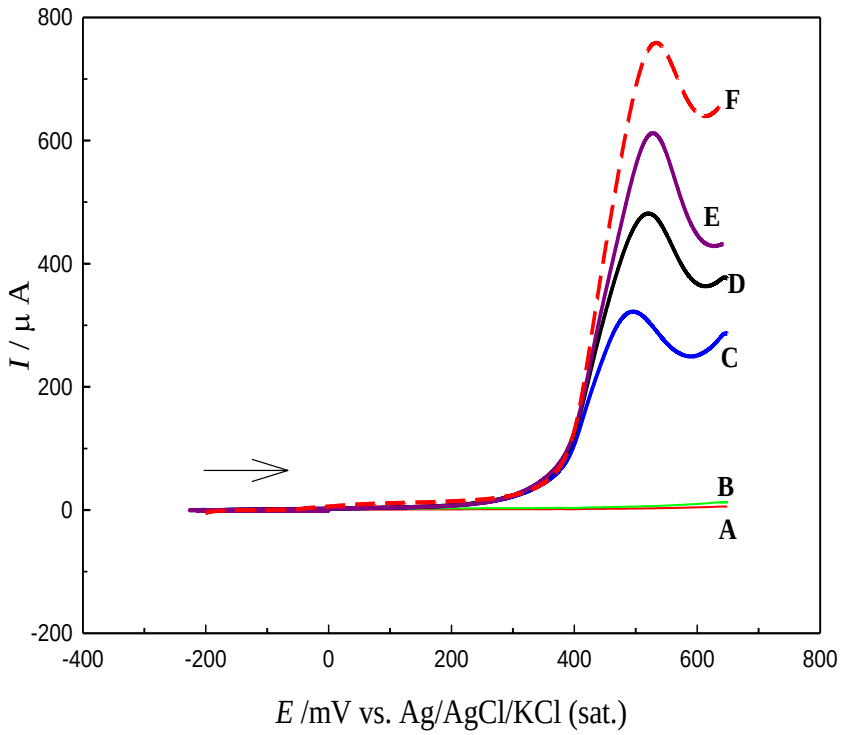

Figure 9. LSV in 0.5 M NaOH solution containing of 20 mM glucose. The scan rate is 100 mV s^{-1} at GC (A), $GC_{OX\text{-}AC}$ (B), GC/NiO_x (C) and $GC_{OX\text{-}AC}/NiO_x$ (D-F) where GC was pretreated by oxidation for 300 s at 1 (D), 1.5 (E) and 2 V (F) in 0.1 M H_2SO_4.

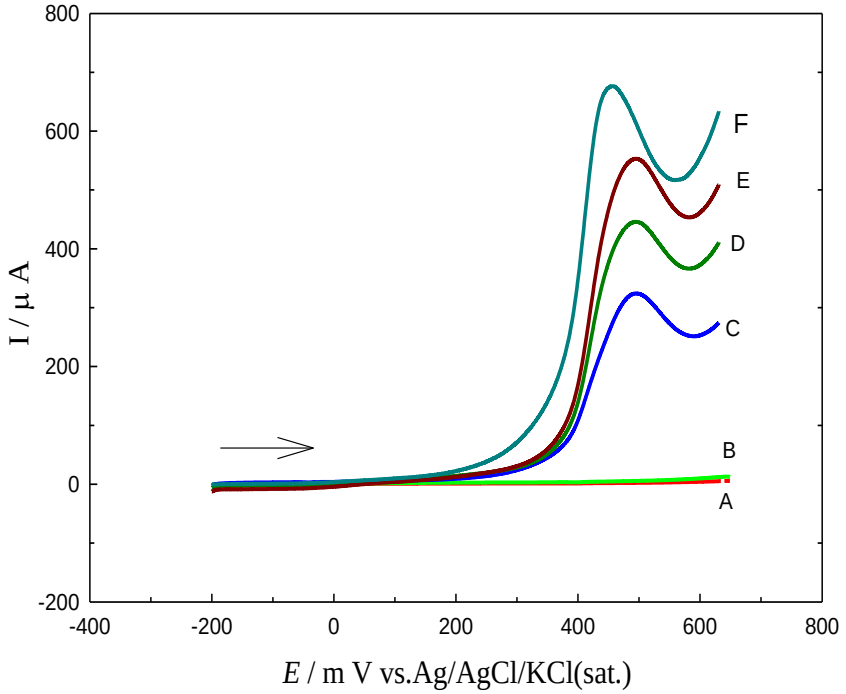

Figure 10. LSV in 0.5 M NaOH solution containing of 20 mM of glucose. The scan rate is 100 mV s^{-1} at GC (A), GC_{OX-AL} (B), GC/NiO_x (C), GC_{OX-AL}/NiO_x (D-F) where GC was pretreated by oxidation for 300 s at 1V(D), 1.5 (E) and 2V (F) in 0.1 M NaOH.

Table 4 lists the values of I_p and E_p extracted such LSVs at the different electrodes and conditions (different E_{anodic} and t_{anodic} of GC oxidation). The results point to the enhancement of the glucose electrooxidation upon anodic oxidation of GC in acidic and alkaline solutions. The increase in E_{anodic} and/or t_{anodic} results in an increase in the peak current of glucose oxidation. The increase in I_p for GC_{OX-AC}/NiO_x is more pronounced than that for GC_{OX-AL}/NiO_x. However, GC_{OX-AL}/NiO_x shows a negative shift in the peak and onset potentials for glucose oxidation. This may be attributed to the impacts of the different shape and size of the NiO_x nanoparticles as discussed in Figs. 2 and 3 (see also Tables 1-3).

The above conclusions cannot be correlated to a possible different loadings of the NiO_x since fixed amount of charge (15 mC) is passed during the Ni electrodeposition on either GC or GC_{OX-AC} or GC_{OX-AL} at any conditions (see Table 2) (see discussion in the previous section). That is to say, the improvement in the electrochemical activity of GC_{OX-AC}/NiO_x or GC_{OX-AL}/NiO_x towards glucose oxidation was not attributed to different loadings of NiO_x. It rather, to the surface oxidation the GC and the consequent changes in the structural characteristics of the of the NiO_x nanoparticles. It is concluded that the enhancement is attributed to the increase in the substrate (GC) surface area. This results in a better exposure to the NiO_x nanoparticles for glucose oxidation. As revealed from the SEM images in Fig. 3, the size of NiO_x nanoparticles on GC_{ox} is lower than that deposited on the untreated GC. The decrease in the size of the NiO_x nanoparticles is accompanied by an increase in its surface area and hence an increase in the peak current of glucose oxidation. Also, a possible synergism between NiO_x

and the newly generated C-O functional groups exist. Further possibility is the preferable deposition of active β-NiOOH rather than less active γ-NiOOH.

An attempt to correlate the modification that took place on the electrochemical characteristics of the $Ni(OH)_2$/NiOOH redox couple (see Table 3) with the enhancement in glucose oxidation (see Table 4) can derive us to the following remarks. The enhancement in the glucose oxidation is affected by the increase in the peak current of the Ni^{2+}/Ni^{3+} couple and the surface concentration of the active Ni species. It rather and to some extent does not depend on the ratio (I_{pc}/I_{pa}). That is to say, the enhancement depends mainly on the amount of the active Ni species and to little extent on its reversibility. The disappearance of the cathodic peak of the conversion NiOOH→ $Ni(OH)_2$ from the cathodic scan (not shown in the LSV of Fig. 6) is an evidence of the role of the Ni^{3+} concentration on the oxidation of glucose by what is well known electrocatalytic mechanism.

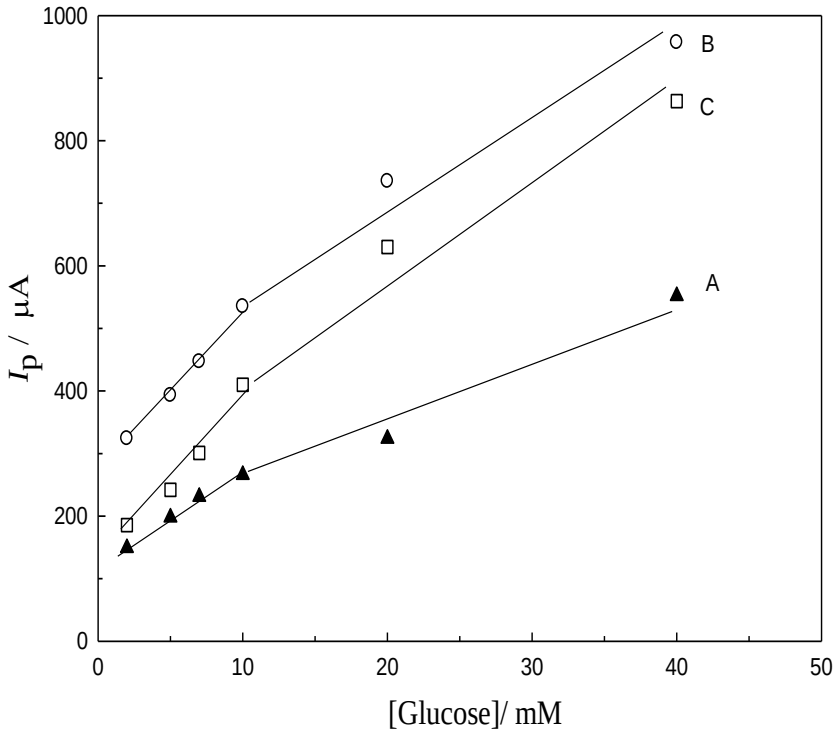

Figure 11. The relations between the peak current, I_p and the [glucose] at GC/NiO_x (A), $GC_{OX\text{-}AC}/NiO_x$ (B) and $GC_{OX\text{-}AL}/NiO_x$ (C).

The effect of glucose concentration was studied by taking different CVs for glucose oxidation at different glucose concentrations on the different electrodes (GC/NiO_x, $GC_{OX\text{-}AC}$ /NiO_x and $GC_{OX\text{-}AL}$ /NiO_x) at scan rate of 100 mV s^{-1} at the same potential range shown in Figs. 6-8. The peak current was recorded and plotted as a function of [glucose] as shown in Fig. 11. The figure shows the above relation between I_p and [glucose] in the range of 2-40 mM. As the concentration increases, the peak current increases linearly at [glucose] ≤ 10 mM. The fact that the rate of glucose oxidation increases with the [glucose] indicates that glucose oxidation on all the three electrodes is a typical electrocatalytic response. It can be suggested that the above relation of I_p and [glucose] is due to a diffusion-controlled process and yet diffusion plays an important role at the concentration range ≤ 10 mM.

Tafel plots were taken for glucose oxidation from 20 mM glucose oxidation on GC/NiO_x (A), GC_{OX-AC} /NiO_x (B) and GC_{OX-AL} /NiO_x (C) using scan rate of 5 mV s^{-1} are given in Fig. 12. The plots confirm the enhancement of the glucose oxidation on GC_{OX-AC} /NiO_x (B) and GC_{OX-AL}/NiO_x (C) compared to GC/NiO_x (A). Tafel slopes estimated from the plots are 118, 125 and 129 mV/dec for GC/NiOx, GC_{OX-AC} /NiO_x and GC_{OX-AL}/NiO_x, respectively. The comparable and closer values of the above Tafel slopes indicate that the mechanism of glucose oxidation does not change on all electrodes and it is one-electron controlled process (see Eq. 4). As proposed by some authors, conversion of Ni(II) to Ni(III) via its redox transition is followed by glucose oxidation on the modified surface via the following reaction: [41-44]

$$\mathrm{Ni(III)} + \mathrm{glucose} \rightarrow \mathrm{intermdiate} + \mathrm{Ni(II)} \quad (4)$$

$$\mathrm{Ni(III)} + \mathrm{intermdiate} \rightarrow \mathrm{products} + \mathrm{Ni(II)} \quad (5)$$

Where Ni^{3+} sites are regenerated by the power source. The above mechanism does not completely exclude direct electrooxidation of glucose on the NiO_x surface [45,46].

Discussion of the above results and conclusions may be presented here. One of these conclusions is: the enhancement of the glucose oxidation on either GC_{OX-AC} /NiO_x or GC_{OX-AL}/NiO_x compared to GC/NiO_x. Generally, the enhancement is attributed to the increase in the substrate (GC) surface area which gives rise to a better exposure of the NiO_x nanoparticles to glucose oxidation. As shown in Fig. 2 the roughness and hence the surface area of GC_{OX-AC} is higher than GC_{OX-AL}. As revealed from the SEM images in Fig. 3, the size of the NiO_x nanoparticles on either GC_{OX-AC} or GC_{OX-AL} is lower than that deposited on the untreated GC. The decrease in the size of the NiO_x nanoparticles is accompanied by an increase in its surface area and hence an increase in the peak current of glucose oxidation. As evident from Fig. 5 and Table 3, there is an obvious enhancement of the redox $Ni(OH)_2$/NiOOH system as understood from the higher peak currents, reversibility and increase of the surface concentration of Ni active sites. The enhancement of the glucose oxidation follows the enhancement of the $Ni(OH)_2$/NiOOH couple.

It is well documented in literature [47] that graphitic, phenolic and carboxylic groups are the main functional groups upon anodic oxidation of GC. This can lower the possibility of poisoning from the oxidation products of glucose and hence higher currents for glucose oxidation were obtained on either GC_{OX-AC}/NiO_x or GC_{OX-AL}/NiO_x. Higher adsorption of glucose on the more hydrophilic surface (GC_{ox}) is also another factor.

It is well documented in literature that anodic oxidation of GC in acid or alkali results in an increase of the percentage surface composition of C-O functional groups bearing –OH group. For instance see XPS work performed by one of the author (Saleh) in Ref. [47], and other important work by Jovanovic *et al*. [28-30] The electrocatalytic oxidation of glucose [48,49] and other small organic molecules such as methanol [50] is enhanced by the presence of –OH group adsorbed on the GC surface (i.e., OH_{ads}). According to Ref. [6] the percentage of OH-containing groups resulting from anodic oxidation in acid is higher than that obtained from oxidation in alkali. Less particle size of NiO_x (see Fig. 2) offers more active sites closely located to –OH like groups on the oxidized GC. Thus, the effect of OH-like groups participating in the oxidation of the adsorbed intermediates must be

much higher and therefore the activity of GC_{ox}/NiO_x electrode must be remarkably increased for glucose oxidation in comparison with GC/NiO_x.

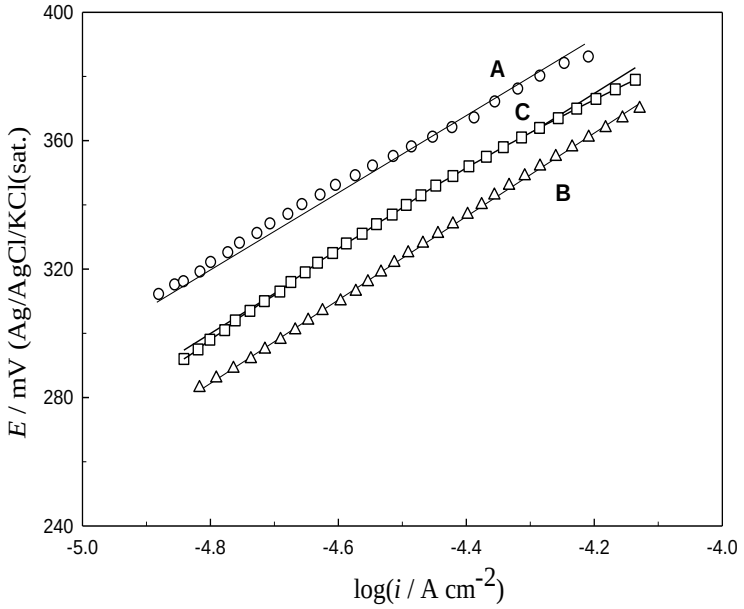

Figure 12. Tafel plots for GC/NiO_x (A), GC_{OX-AC}/NiO_x (B) and GC_{OX-AL}/NiO_x (C) electrodes in 0.5 M NaOH solution containing 20 mM glucose at a scan rate 5 mV/s.

The work done in Ref. [30], demonstrated that the major functional groups on GC surface are phenolic, carboxyl and carbonyl. Studies of XPS for an oxidized GC in H_2SO_4 showed the increase in the fraction of all C-O functional groups with highest increase of phenolic and carboxyl groups and lowest increase of carbonyl group. Accordingly, the higher percentage of acidic groups on oxidized GC should promote the higher fraction of oxygen containing species in the NiO_x catalyst than in the NiO_x deposited on the polished GC. Consequently, GC_{OX-AC}/NiO_x or GC_{OX-AL}/NiO_x are more active in glucose oxidation in comparison with GC/NiO_x.

In another remark, while smaller particle size of NiO_x obtained on GC_{OX-AC} and higher surface area of GC_{OX-AC} (higher roughness, see Fig. 2) compared to GC_{OX-AL} implements higher peak currents of glucose oxidation on either GC_{OX-AC}/NiO_x, the adsorbed –OH groups on the GC_{OX-AL} (coming from NaOH during anodic oxidation in the NaOH) maybe the reason of the negative shift in both E_p and E_{onset} of glucose oxidation on the GC_{OX-AL}/NiO_x. The role of adsorbed –OH group in catalyzing the electrooxidation of organic molecules is reported in literatures [51,52].

4. CONCLUSIONS

Effects of anodic oxidation of GC in acid and alkali on the electrodeposition of NiO_x and on the electrocatalytic activity of the NiO_x were studied. The anodic pretreatment of the GC electrode was achieved at different anodic potentials and different time periods. The shape and size of the NiO_x

nanoparticles and the time required for NiO_x electrodeposition is affected by the anodic oxidation of the GC electrode. The pretreatment of GC by anodic oxidation has its impact on the redox couple of NiO_x, i.e., on the $Ni(OH)_2 \leftrightarrow NiOOH$. This was attributed to the increase in the GC surface area and in the concentration of C-O functional groups. Glucose electrooxidation is enhanced on either GC_{OX-AC}/NiO_x or GC_{OX-AL}/NiO_x compared to GC/NiO_x. While both GC_{OX-AC}/NiO_x and GC_{OX-AL}/NiO_x support high I_p of glucose oxidation, GC_{OX-AL}/NiO_x shifts the E_p and E_{onset} to more negative values. The above conclusions were generally discussed in the light of the obtained surface and electrochemical analysis. However, further work has to be done (e.g., XPS study) for further explanation of the above conclusions.

References

1. G.K. Kiema, M. Aktay, M.T. McDermott, *J. Electroanal. Chem*. 540 (2003) 7.
2. J. Premkumer, S.B. Khoo, *Elecrochem. Commun*., 6 (2004) 984.
3. G. Ilangovan, K.C. Pillai, *J. Electroanal. Chem*., 431 (1997)11.
4. Y. Yang, Z. Lin, *Synth. Met*. 78 (1996) 111.
5. K. Shi, K. Keung Shiu, *Anal. Chem*., 74 (2002) 879.
6. A. Dekanski, J. Stevanovic, R. Stevanovic, B. Z. Nikolic, V.M. Jovanovic, *Carbon*, 39 (2001) 1195.
7. A. Dekanski, J. Stevanovic, R. Stevanovic, V.M. Jovanovic, *Carbon*, 39 (2001) 1207.
8. W. Xing, F. Li, Z. Yan, G. Lu, *J. Power Sources*, 134 (2004) 324.
9. Mao-Sung Wu, H-Ho Hsieh, *Electrochim. Acta*, 53 (2008) 3427.
10. A. El-Shafei, *J. Electroanal. Chem*., 471 (1999) 89.
11. M. Rahim, R. Hameed, M. Khalil, *J. Power Sources*, 134 (2004) 160.
12. G. Snook, N. Duffy, A. Pandolfo, *J. Electrochem. Soc*., 155(2008) A262.
13. Y. Hu, J. Jin, P. Wu, H. Zhang and C. Cai, *Electrochim. Acta*, 56 (2010) 491.
14. S.-Y. Kwon, H.-D. Kwen and S.-H. Choi, *J. Sensors*, 2012 (2012) 8.
15. S. Hui, J. Zhang, X. Chen, H. Xu, D. Ma, Y. Liu and B. Tao, *Sens. Act. B: Chemical*, 155 (2011) 592.
16. J. L. Garcia-Miquel, Q. Zhang, S. J. Allen, A. Rougier, A. Blyr, H.O. Davies, A.C. Jones, T. J. Leedham, P. A.William, S. A. Impey, *Thin Solid Films*, 424 (2003) 165.
17. I. Danaee, M. Jafarian, F. Forouzandeh, F. Gobal, M.G. Mahjani, *Electrochim. Acta*, 53(2008) 6602.
18. Z. Luo, S. Yin, K. Wang, H. Li, L. Wang, H. Xu, J. Xia, *Mat. Chem.Phys*., 132 (2012) 387.
19. Y. Ding, Y. Liu, J. Parisi, L. Zhang, Y. Lei, *Biosen. Bioelectron*., 28 (2011) 392.
20. R.N. Singh, A. Singh, A.Nintida, D. Mishra, *Int. J. Hyd. Energy*, 33 (2008) 6878.
21. N. Spinner, W. E. Mustain, , *Electrochim. Acta*, 56 (2011) 5656.
22. A.M. Ghonim, B.E. El-Anadouli, M.M. Saleh, *Electrochimica Acta* 114 (2013) 713.
23. Z. Luob, S.Yin, K. Wang, H. Li, L. Wang, H. Xu, J. Xia, *Mat. Chem. Phys*.,132 (2012) 387.
24. M. Vidotti, C.D. Cerri, R.F. Carvalhal, J.C. Dias, R.K. Mendes, S.I. Córdoba de Torresi, L.T. Kubota, *J. Electroanal. Chem*., 636 (2009) 18.
25. V. Ganesh, D. Latha Maheswari and S. Berchmans, *Electrochim. Acta*, 56 (2011) 1197.
26. D.E. Pissinis, L.E. Sereno, J.M. Marioli, *J. Electroanal. Chem*., 694 (2013) 23.
27. Q.-Ling Zhao, Zhi-L. Zhang, L. Bao, Dai-W Pang, *Electrochem. Comm*., 10 (2008) 181.
28. V. M. Jovanovic, S. Terzic, A.V. Tripkovic, K.D. Popovic, J.D. Lov, *Electrochem. Comm*., 6 (2004) 1254.

29. V. M. Jovanovic, D. Tripkovic, A. Tripkovic, A. Kowal, J. Stoch, *Electrochem. Comm*., 7 (2005) 1039.
30. S. Stevanovic, V. Panic, D. Tripkovic, V. M. Jovanovic, *Electrochem. Comm*., 11 (2009) 18.
31. R.C. Engstrom, *Anal. Chem*. 54 (1982) 2310.
32. R.D. Engstrom, V.A. Strasser, *Anal. Chem*. 56 (1984) 136.
33. S.M. El-Refaei, M.I. Awad, B.E. El-Anadouli, M.M. Saleh, *Electrochim. Acta*, 92 (2013) 460.
34. H. Bode, K. Dehmelt and J. Witte, *Electrochim. Acta*, 11 (1966) 1079.
35. A.J. Bard, L. R. Faulkner, *Electrochemical methods: fundamentals and applications*. New York: Wiley; 1980.
36. M. M. Saleh, C. Weilich, K.-M. Mangold, K. Juttner, *J. Applied Electrochem*., 36 (2006)179.
37. R.S. Schrebler Guzman, J.R. Vilche, A.J. Arvia, *J. Electrochem. Soc*. 125 (1978) 1578.
38. D. Giovanelli, N.S. Lawrence, L. Jiang, T.G.J. Jones, R.G. Compton, *Sens. Actuators, B: Chem*., 88 (2003) 320.
39. R. Vittal, H. Gomathi, G. Prabhakara Rao, *J. Electroanal. Chem*., 497 (2001) 47.
40. J. Joseph, H. Gomathi, G. Prabhakara Rao, *Electrochim. Acta*, 36 (1991)1531.
41. S.M. El-Refaei, M.M. Saleh, M.I. Awad, *J. Power Sources* 223 (2013) 125.
42. M. Fleischmann, K. Korinek, D. Pletcher, *J. Electroanal. Chem. Int. Electrochem*., 31 (1971) 39.
43. J. Taraszewska, G. Rosłonek, *J. Electroanal. Chem*. 364 (1994) 209.
44. J.R. Allen, A. Florido, S.D. Young, S. Daunert, L.G. Bachas, *Electroanalysis*, 7, (1995) 710.
45. I. Danaee, M. Jafarian, F. Forouzandeh, F. Gobal, M.G. Mahjani, *Int. J. Hydrogen Energy*, 33 (2008) 4367.
46. I. Danaee, M. Jafarian, A. Mirzapoor, F. Gobalb, M.G. Mahjani, *Electrochim. Acta*, 55 (2010) 2093.
47. M. M. Saleh, M.I. Awad, T. Okajima, K. Suga, T. Ohsaka, *Electrochim. Acta*, 52, 3095 (2007).
48. Y. B. Vassilyev, O.A. Khazova, N.N. Nikolaeva, *J. Electroanal. Chem*., 196 (1985) 127.
49. M. W. Hsiao, R.R. Adzic, E.B. Yeager, *Electrochim. Acta*, 37 (1992) 357.
50. S. Stevanovic, V. Panic, D. Tripkovic, V.M. Jovanovic, *Electrochem. Commun*., 11 (2009) 18.
51. I. G. Casella, M. R. Guascito, M. G. Sannazzaro, *J. Electroanal. Chem*., 462 (1999) 202.
52. V. Vedharathinam, G. G. Botte, *Electrochim. Acta*, 81 (2012) 292.